	vaccine antigen					non-vaccine antigen										
	Gag				Vif	Vpr	Tat					Rev		Nef		
	165	333	375	376	143	73	23	115	120	122	125	45	50	63	100	124
wk 5																
R- 421					++											
R- 431					+											
R- 438	++		+							++						
wk 12																
R- 421		++			++				+		+	+	+			++
R- 431					+		+			++						
R- 438	++			++		+		++						++	++	

Fig. 4. Viral mutations in DNA-vaccinated macaques. Plasma viral genome sequencing was performed as described previously [18] to determine mutations resulting in amino acid substitutions in SIV Gag, Pol, Vif, Vpx, Vpr, Tat, Rev, and Nef antigens (except for Env) at weeks 5 and 12 in DNA-vaccinated macaques. The amino acid positions showing mutant sequences dominantly (++) or equivalently with wild type (+) are shown. While we found a mutation leading to a lysine-to-arginine alteration at the 40th amino acid in Rev in all animals, this mutation is not shown because the wild-type sequence at this position in the SIVmac239 molecular clone is considered to be a suboptimal nucleotide that frequently reverts to an alternative sequence in vivo [18,23].

IFN-γ monoclonal antibodies (Becton Dickinson). Specific $CD8^+$ T-cell levels were calculated by subtracting nonspecific IFN-γ^+ $CD8^+$ T-cell frequencies from those after Gag-specific, pseudotyped SIV-specific, or peptide-specific stimulation. Specific $CD8^+$ T-cell levels lower than 100 per million PBMCs were considered negative.

3. Results and discussion

In our previous SIVmac239 challenge experiments, the prophylactic DNA/SeV-Gag vaccination did not result in viral control in rhesus macaques possessing the MHC-I haplotype *90-088-Ij*. These vaccinated animals showed similar levels of plasma viral loads as those in unvaccinated *90-088-Ij*-positive animals after SIV challenge (Fig. 1A). Analysis of virus-specific $CD8^+$ T-cell responses using PBMCs at week 2 after challenge showed equivalent Gag-specific and pseudotyped SIV-specific (Gag-, Pol-, Vif-, and Vpx-specific) CTL responses in all three vaccinees (Fig. 1B). Pseudotyped SIV-specific CTL responses were also detected in all three unvaccinated animals, but Gag-specific CTL responses were undetectable in two out of the three; even the Gag-specific CTL responses detected in macaque R04-014 were much lower than pseudotyped SIV-specific CTL responses, indicating dominant induction of CTL responses specific for SIV antigens other than Gag (Fig. 1B). Thus, in the acute phase of SIV infection, SIV non-Gag antigen-specific CTL responses were dominantly induced in unvaccinated *90-088-Ij*-positive macaques, whereas vaccine antigen (Gag)-specific CTL responses were dominant in *90-088-Ij*-positive vaccinees.

We then analyzed another vaccinees that failed to control a SIVmac239 challenge; these macaques were vaccinated with SeV-Gag alone or DNA alone. First, we compared post-challenge CTL responses in unvaccinated and SeV-Gag-vaccinated macaques possessing the MHC-I haplotype *90-120-Ib*. Both macaques failed to control SIV replication after challenge (Fig. 2A). In the unvaccinated animal R06-001, Gag-specific CTL responses were undetectable but pseudotyped SIV-specific CTL responses were induced efficiently at weeks 2 and 12 (Fig. 2B). In contrast, Gag-specific CTL responses were induced efficiently at week 2 in the SeV-Gag-vaccinated animal R05-028 (Fig. 2B). At week 12, Gag-specific CTL responses became undetectable while pseudotyped SIV-specific CTL responses were still detectable in this animal. These results indicate that, in the acute phase after SIVmac239 challenge, the unvaccinated *90-120-Ib*-positive macaque dominantly elicited SIV non-Gag antigen-specific CTL responses whereas the SeV-Gag-vaccinated *90-120-Ib*-positive macaque dominantly induced vaccine antigen (Gag)-specific CTL responses.

Next, we analyzed post-challenge CTL responses in three DNA-vaccinated macaques. These animals failed to control SIVmac239 replication after challenge (Fig. 3A). The DNA used for the vaccination and the pseudotyped SIV genome both have the same SIVmac239-derived region encoding Gag, Pol, Vif, and Vpx, thus expected to induce pseudotyped SIV-specific CTL responses. Pseudotyped SIV-specific CTL responses, namely vaccine antigen-specific CTL responses, were induced efficiently at week 2 but diminished after that in all three animals (Fig. 3B). In contrast, Tat/Rev- and Nef-specific CTL responses were undetectable at week 2 but induced later (Fig. 3B). Again, vaccine antigen-specific CTL responses were dominantly induced in the acute phase after SIV challenge and non-vaccine antigen-specific CTL responses were elicited later.

All three animals showed viral genome mutations leading to amino acid substitutions in Gag or Vif at week 5 (Fig. 4). Further analysis indicated that viral mutations in vaccine antigen-coding regions appeared earlier than those in other regions. These results may reflect selective pressure on SIV by vaccine antigen-specific CTL responses dominantly induced in the acute phase, although it remains undetermined whether these mutations are CTL escape ones. Disappearance of vaccine antigen-specific CTL responses at week 12 may be explained by rapid selection of CTL escape mutations in vaccine antigen-coding regions. However, analysis using peptides found Gag-specific CTL responses in macaques R-421 and R-431 that had no gag mutations at week 5 (data not shown), suggesting involvement of immunodominance [20] in the disappearance of vaccine antigen-specific CTL responses at week 12.

In summary, the present study indicates that vaccine antigen-specific CTL responses are induced dominantly in the acute phase after viral exposure, with delayed induction of CTL responses specific for SIV non-vaccine antigens (SIV antigens other than vaccine antigens). While this delay previously-observed in vaccine-based SIV controllers [10] can be explained not only by immunodominance but also by reduction in viral loads, the delay

Please cite this article in press as: Y. Takahara et al., Dominant induction of vaccine antigen-specific cytotoxic T lymphocyte responses after simian immunodeficiency virus challenge, Biochem. Biophys. Res. Commun. (2011), doi:10.1016/j.bbrc.2011.04.071

in vaccinated non-controllers in the present study might reflect the immunodominance in CTL responses. Thus, in development of a prophylactic, CTL-inducing AIDS vaccine, it is important to select vaccine antigens leading to effective CTL responses post-viral exposure [21,22]. These results imply a significant influence of prophylactic vaccination on the immunodominance pattern of CTL responses post-viral exposure, providing insights into antigen design in development of a CTL-inducing AIDS vaccine.

Acknowledgments

This work was supported by Grants-in-aid from the Ministry of Education, Culture, Sports, Science, and Technology, Grants-in-aid from the Ministry of Health, Labor, and Welfare, and a Grant from Takeda Science Foundation in Japan.

References

[1] R.A. Koup, J.T. Safrit, Y. Cao, C.A. Andrews, G. McLeod, W. Borkowsky, C. Farthing, D.D. Ho, Temporal association of cellular immune responses with the initial control of viremia in primary human immunodeficiency virus type 1 syndrome, J. Virol. 68 (1994) 4650–4655.

[2] P. Borrow, H. Lewicki, B.H. Hahn, G.M. Shaw, M.B. Oldstone, Virus-specific CD8+ cytotoxic T-lymphocyte activity associated with control of viremia in primary human immunodeficiency virus type 1 infection, J. Virol. 68 (1994) 6103–6110.

[3] T. Matano, R. Shibata, C. Siemon, M. Connors, H.C. Lane, M.A. Martin, Administration of an anti-CD8 monoclonal antibody interferes with the clearance of chimeric simian/human immunodeficiency virus during primary infections of rhesus macaques, J. Virol. 72 (1998) 164–169.

[4] X. Jin, D.E. Bauer, S.E. Tuttleton, S. Lewin, A. Gettie, J. Blanchard, C.E. Irwin, J.T. Safrit, J. Mittler, L. Weinberger, L.G. Kostrikis, L. Zhang, A.S. Perelson, D.D. Ho, Dramatic rise in plasma viremia after CD8(+) T cell depletion in simian immunodeficiency virus-infected macaques, J. Exp. Med. 189 (1999) 991–998.

[5] P.J. Goulder, D.I. Watkins, HIV and SIV CTL escape: implications for vaccine design, Nat. Rev. Immunol. 4 (2004) 630–640.

[6] T. Matano, M. Kano, H. Nakamura, A. Takeda, Y. Nagai, Rapid appearance of secondary immune responses and protection from acute CD4 depletion after a highly pathogenic immunodeficiency virus challenge in macaques vaccinated with a DNA prime/Sendai virus vector boost regimen, J. Virol. 75 (2001) 11891–11896.

[7] T. Matano, M. Kobayashi, H. Igarashi, A. Takeda, H. Nakamura, M. Kano, C. Sugimoto, K. Mori, A. Iida, T. Hirata, M. Hasegawa, T. Yuasa, M. Miyazawa, Y. Takahashi, M. Yasunami, A. Kimura, D.H. O'Connor, D.I. Watkins, Y. Nagai, Cytotoxic T lymphocyte-based control of simian immunodeficiency virus replication in a preclinical AIDS vaccine trial, J. Exp. Med. 199 (2004) 1709–1718.

[8] Y. Takahashi-Tanaka, M. Yasunami, T. Naruse, K. Hinohara, T. Matano, K. Mori, M. Miysazawa, M. Honda, Y. Yasutomi, Y. Nagai, A. Kimura, Reference strand-mediated conformation analysis (RSCA)-based typing of multiple alleles in the rhesus macaque MHC class I Mamu-A and Mamu-B loci, Electrophoresis 28 (2007) 918–924.

[9] M. Kawada, T. Tsukamoto, H. Yamamoto, N. Iwamoto, K. Kurihara, A. Takeda, C. Moriya, H. Takeuchi, H. Akari, T. Matano, Gag-specific cytotoxic T lymphocyte-based control of primary simian immunodeficiency virus replication in a vaccine trial, J. Virol. 82 (2008) 10199–10206.

[10] T. Tsukamoto, A. Takeda, T. Yamamoto, H. Yamamoto, M. Kawada, T. Matano, Impact of cytotoxic-T-lymphocyte memory induction without virus-specific CD4+ T-Cell help on control of a simian immunodeficiency virus challenge in rhesus macaques, J. Virol. 83 (2009) 9339–9346.

[11] H. Yamamoto, M. Kawada, A. Takeda, H. Igarashi, T. Matano, Post-infection immunodeficiency virus control by neutralizing antibodies, PLoS ONE 2 (2007) e540.

[12] R. Shibata, F. Maldarelli, C. Siemon, T. Matano, M. Parta, G. Miller, T. Fredrickson, M.A. Martin, Infection and pathogenicity of chimeric simian-human immunodeficiency viruses in macaques: determinants of high virus loads and CD4 cell killing, J. Infect. Dis. 176 (1997) 362–373.

[13] H.O. Li, Y.F. Zhu, M. Asakawa, H. Kuma, T. Hirata, Y. Ueda, Y.S. Lee, M. Fukumura, A. Iida, A. Kato, Y. Nagai, M. Hasegawa, A cytoplasmic RNA vector derived from nontransmissible Sendai virus with efficient gene transfer and expression, J. Virol. 74 (2000) 6564–6569.

[14] A. Takeda, H. Igarashi, H. Nakamura, M. Kano, A. Iida, T. Hirata, M. Hasegawa, Y. Nagai, T. Matano, Protective efficacy of an AIDS vaccine, a single DNA priming followed by a single booster with a recombinant replication-defective Sendai virus vector, in a macaque AIDS model, J. Virol. 77 (2003) 9710–9715.

[15] H.W. Kestler 3rd, D.J. Ringler, K. Mori, D.L. Panicali, P.K. Sehgal, M.D. Daniel, R.C. Desrosiers, Importance of the nef gene for maintenance of high virus loads and for development of AIDS, Cell 65 (1991) 651–662.

[16] T. Matano, M. Kano, T. Odawara, H. Nakamura, A. Takeda, K. Mori, T. Sato, Y. Nagai, Induction of protective immunity against pathogenic simian immunodeficiency virus by a foreign receptor-dependent replication of an engineered avirulent virus, Vaccine 18 (2000) 3310–3318.

[17] L.M. Albritton, L. Tweng, D. Scadden, J.M. Cunningham, A putative murine retrovirus receptor gene encodes a multiple membrane-spanning protein and confers susceptibility to virus infection, Cell 57 (1989) 659–666.

[18] M. Kawada, T. Tsukamoto, H. Yamamoto, A. Takeda, H. Igarashi, D.I. Watkins, T. Matano, Long-term control of simian immunodeficiency virus replication with central memory CD4+ T-cell preservation after nonsterile protection by a cytotoxic T-lymphocyte-based vaccine, J. Virol. 81 (2007) 5202–5211.

[19] N. Iwamoto, T. Tsukamoto, M. Kawada, A. Takeda, H. Yamamoto, H. Takeuchi, T. Matano, Broadening of CD8+ cell responses in vaccine-based simian immunodeficiency virus controllers, AIDS 24 (2010) 2777–2787.

[20] S. Tenzer, E. Wee, A. Burgevin, G. Stewart-Jones, L. Friis, K. Lamberth, C.H. Chang, M. Harndahl, M. Weimershaus, J. Gerstoft, N. Akkad, P. Klenerman, L. Fugger, E.Y. Jones, A.J. McMichael, S. Buus, H. Schild, P. van Endert, A.K. Iversen, Antigen processing influences HIV-specific cytotoxic T lymphocyte immunodominance, Nat. Immunol. 10 (2009) 636–646.

[21] P.J.R. Goulder, D.I. Watkins, Impact of MHC class I diversity on immune control of immunodeficiency virus replication, Nat. Rev. Immunol. 8 (2008) 619–630.

[22] H. Streeck, J.S. Jolin, Y. Qi, B. Yassine-Diab, R.C. Johnson, D.S. Kwon, M.M. Addo, C. Brumme, J.P. Routy, S. Little, H.K. Jessen, A.D. Kelleher, F.M. Hecht, R.P. Sekaly, E.S. Rosenberg, B.D. Walker, M. Carrington, M. Altfeld, Human immunodeficiency virus type 1-specific CD8+ T-cell responses during primary infection are major determinants of the viral set point and loss of CD4+ T cells, J. Virol. 83 (2009) 7641–7648.

[23] L. Alexander, L. Denekamp, S. Czajak, R.C. Desrosiers, Suboptimal nucleotides in the infectious, pathogenic simian immunodeficiency virus clone SIVmac239, J. Virol. 75 (2001) 4019–4022.

Immunogenetics
DOI 10.1007/s00251-011-0531-y

ORIGINAL PAPER

ULBP4/RAET1E is highly polymorphic in the Old World monkey

Taeko K. Naruse · Yukiko Okuda · Kazuyasu Mori · Hirofumi Akari · Tetsuro Matano · Akinori Kimura

Received: 22 February 2011 / Accepted: 21 April 2011

Abstract Natural-killer group 2 member D (NKG2D) is an activating receptor that plays an important role in the immune response mediated by NK cells, $\gamma\delta^+$ T cells, and $CD8^+$ T cells. In humans, MHC class I chain-related genes and UL-16 binding protein (ULBP)/retinoic acid early transcript 1 (REAT1) gene family encode ligands for NKG2D. The rhesus and crab-eating macaques, which belong to the Old World monkeys, are widely used as non-human primate models in medical researches on the immunological process. In the present study, we investigated the polymorphisms of *ULBP4/RAET1E*, a member of the *ULBP/RAET1* family, and found 25 and 14 alleles from the rhesus and crab-eating macaques, respectively, of which diversities were far more extended than in humans. A phylogenetic study suggested that the allelic diversification of ULBP4/RAET1E predated the divergence of rhesus and crab-eating macaques.

T. K. Naruse · A. Kimura (✉)
Department of Molecular Pathogenesis, Medical Research Institute, Tokyo Medical and Dental University,
1-5-45 Yushima, Bunkyo-ku,
Tokyo 113–8510, Japan
e-mail: akitis@mri.tmd.ac.jp

Y. Okuda · A. Kimura
Laboratory of Genome Diversity, Graduate School of Biomedical Science, Tokyo Medical and Dental University,
Tokyo, Japan

K. Mori · T. Matano
AIDS Research Center, National Institute of Infectious Diseases,
Tokyo, Japan

H. Akari
Primate Research Institute, Kyoto University,
Inuyama, Japan

T. Matano
International Research Center for Infectious Diseases,
The Institute of Medical Science, The University of Tokyo,
Tokyo, Japan

Published online: 07 May 2011

Keywords Rhesus macaque · Crab-eating macaque · ULBP4/RAET1E · NKG2D · Polymorphism

Introduction

Non-human primates, such as rhesus and crab-eating macaques, are important animal models for the study of infectious diseases, autoimmune diseases, and organ transplantation. These macaques are members of the Old World monkeys, and it has been reported that the genetic diversity in the rhesus macaque is quite unique, that is, more than 60% of the rhesus macaque-specific expansions are found in the protein coding sequences (Gibbs et al. 2007). To evaluate the results of immunological experiments in the macaque models, it is essential to characterize the genetic diversity of immune-related molecules which may control the individual differences in the immune response against foreign antigens and/or pathogens. It has been reported that the gene copy number in the major histocompatibility complex (MHC) loci in the rhesus and crab-eating macaques is higher than that in humans (Kulski et al. 2004; Gibbs et al. 2007; Otting et al. 2007). In addition, the extent of genetic diversity differed, in part, depending on the geographic areas, and we have reported that the diversity of MHC class I genes in the rhesus macaque is considerably different depending on habitat (Naruse et al. 2010).

Because the innate immune system is involved in the response to environmental pathogens, it is necessary to consider the function of natural killer (NK) cells in the experimental animal models. Natural-killer group 2 member D (NKG2D), a C-type lectin molecule, is an activating receptor expressed on the cell surface of NK, $\gamma\delta^+$, and $CD8^+$ T cells, which plays an important role in the immune response (Wu et al. 1999; Raulet 2003). In humans, MHC class I chain-related genes (MIC) and UL-16 binding protein (ULBP)/retinoic acid early transcript 1 (REAT1)

gene family are known to encode ligands for NKG2D (Bauer et al. 1999; Cosman et al. 2001; Chalupny et al. 2003; Bacon et al. 2004). These ligand molecules are usually stress-inducible, and their recognition by NKG2D can lead to the activation of NK cells, consequently killing virus-infected and tumor cells (Pende et al. 2002; Eagle et al. 2006; Pappworth et al. 2007; Ward et al. 2007).

The human *ULBP/RAET1* gene family is located on chromosome 6q24.2, which is composed of ten members including six functional genes, *ULBP1*, *2*, *3*, *4*, *5*, and *6*, corresponding to *RAET1I*, *H*, *N*, *E*, *G*, and *L*, respectively (Radosavljevic et al. 2001; Chalupny et al. 2003; Eagle et al. 2009a, b). In addition, several sequence polymorphisms in each *ULBP* gene have been identified (Romphruk et al. 2009; Antoun et al. 2010). Although it is evident that the cell surface expression of the ligand molecules on target cells is differentially regulated (Eagle et al. 2006), genetic polymorphisms in the coding regions might have a functional impact. We have previously investigated the genetic polymorphisms of *ULBP/RAET1* genes and have found that the *ULBP4/RAET1E* gene is the most polymorphic, with the allelic distribution differing among ethnic groups (Romphruk et al. 2009).

On the other hand, rhesus macaque *ULBP4/RAET1E* (GenBank: NW_001116520) is mapped on the long arm of chromosome 4 (i.e., positions from 31, 164, 822 to 31, 175, 032 of chromosome 4 in the rhesus genome; data obtained from the UCSC Genome Browser at http://genome.ucsc.edu/cgi-bin/hgGateway; Gibbs et al. 2007). However, its genetic polymorphisms are poorly characterized, although the MIC gene polymorphisms are well studied in the rhesus macaque (Seo et al. 1999, 2001; Doxiadis et al. 2007; Averdam et al. 2007). In the present study, we investigated the polymorphisms of *ULBP4/RAET1E* in rhesus and crab-eating macaques. This is the first report demonstrating the extreme diversity of the NKG2D ligand in the Old World monkey.

Materials and methods

Animals

A total of 38 rhesus macaques from seven lineages previously analyzed for the MHC polymorphisms (Naruse et al. 2010) and 24 crab-eating macaques from five lineages were the subjects. They were maintained in the breeding colonies in Japan. The founders of the rhesus macaque colonies were captured in Myanmar and Laos, whereas the founders of crab-eating macaque colonies were captured in Indonesia, Malaysia, and the Philippines. All care, including blood sampling of animals, were in accordance with the guidelines for the Care and Use of Laboratory Animals published by the National Institutes of Health (NIH publication 85–23, revised 1985) and were subjected to prior approval by the local animal protection authority.

DNA extraction and sequencing analysis

Genomic DNAs from B lymphoblastoid cell lines of the rhesus macaque (Naruse et al. 2010) and from whole blood sample of the crab-eating macaque were extracted by using the QuickGene DNA kit (Fujifilm, Tokyo, Japan) according to the manufacturer's instructions. The genomic gene for *ULBP4/RAET1E* of rhesus and crab-eating macaques was amplified by polymerase chain reaction (PCR) with a primer pair designed for the region spanning from introns 1 to 3 of the rhesus gene (NC007861), ULBP4F (5′-TGGGCCTCTTCCCCTGTCC) and ULBP4R (5′-GTGGGAGGTGGGATGGG), using FastStart Taq DNA polymerase (Roche, Mannheim, Germany). The PCR condition was composed of the following steps: denaturation at 95°C for 4 min; 30 cycles of 95°C for 30 s, 63°C for 30 s, and 72°C for 45 s; and additional extension at 72°C for 7 min. The PCR products of about 1,200 bp in length were cloned into pSTBlue-1 AccepTer vector (Novagen, WI, USA) according to the manufacturer's instructions and were transformed to Nova Blue Single™ competent cells (Merck4Biosciences Japan, Tokyo, Japan). Ten to 20 independent transformant colonies were picked up for each sample and subjected to sequencing on both strands by using a BigDye Terminator cycling system and an ABI 3730 automated sequence analyzer (Applied Biosystems, CA, USA).

Data analyses

Nucleotide sequences of *ULBP4/RAET1E* from cloned DNAs were aligned using the Genetyx software package (version 8.0, Genetyx Corp., Japan). If at least three clones from independent PCR or from different individuals showed identical sequences, the sequences were submitted to the DNA Data Bank of Japan (DDBJ). Neighbor-joining trees were constructed with Kimura's 2-parameter method for a phylogenetic analysis of *ULBP4/RAET1E* sequences spanning from exons 2 to 3 including intron 2 by using the Genetyx software. Bootstrap values were based on 5,000 replications. The *ULBP4/RAET1E* sequences from humans (GenBank accession number AY252119), chimpanzees (AY032638), and rhesus (NC007861) were included in the analysis as references.

Structure model analysis

A three-dimensional (3-D) structure model of rhesus ULBP4/RAET1E, with amino acid positions from 1 to 178, was created by a molecular visualization software RasTop2.2 (http://sourceforge.net/projects/rastop/), and the

human RAET1B in complex with NKG2D (Radaev et al. 2001) from the Molecular Modeling Database (MMCB No. 18231) was used as the reference. Polymorphic sites were mapped on the 3-D structure model of macaque RAET1E by using the Cn3D 4.1 program (http://www.ncbi.nlm.nih.gov/Structure/CN3D/cn3d.shtml).

Table 1 Identified alleles of the ULBP4 gene in rhesus and cynomolgus

Species	Allele name	Accession no.	Reference animal	Identical sequence
Rhesus macaque	*Mamu-ULBP4*1.1*	AB568525	R228, R367	
	*Mamu-ULBP4*1.2*	AB568533	R492, R396, R465	
	*Mamu-ULBP4*2*	AB568526	R283, R384, R328, R337	
	*Mamu-ULBP4*3*	AB568527	R346, R361, R396, R379, R408	
	*Mmau-ULBP4*4*	AB568528	R320, R490, R321, R465, R367, R446, R328, R234, R237, R314	
	*Mamu-ULBP4*5*	AB568529	R430, R453, R325, R477, R439, R360, R379, R446, R355	
	*Mamu-ULBP4*6*	AB568530	R437, R350,	
	*Mamu-ULBP4*7.1*	AB568531	R325, R384, R491, R333, R337	
	*Mamu-ULBP4*7.2*	AB568544	R477	
	*Mamu-ULBP4*8*	AB568532	R408, R454, R241, R342, R316	
	*Mamu-ULBP4*9.1*	AB568534	R312, R314	
	*Mamu-ULBP4*9.2*	AB568535	R333	
	*Mamu-ULBP4*10*	AB568536	R316	
	*Mamu-ULBP4*11*	AB568537	R241	
	*Mamu-ULBP4*12*	AB568538	R342	
	*Mamu-ULBP4*13*	AB568539	R491	
	*Mamu-ULBP4*14*	AB568540	R495	*Mafa-ULBP4*1.1*
	*Mamu-ULBP4*15*	AB568541	R350	
	*Mamu-ULBP4*16*	AB568542	R492	
	*Mamu-ULBP4*17*	AB568543	R495	
	*Mamu-ULBP4*18*	AB568545	R454	
	*Mamu-ULBP4*19*	AB568546	R321	
	*Mamu-ULBP4*20*	AB568547	R355	
	*Mamu-ULBP4*21*	AB571025	R437	
	*Mamu-ULBP4*22*	AB571026	R439	
Crab-eating macaque	*Mafa-ULBP4*1.1*	AB578934	M01, P01, P02, C001, C003, C004, C005, C006	*Mamu-ULBP4*14*
	*Mafa-ULBP4*1.2*	AB578935	M02, C004	
	*Mafa-ULBP4*2*	AB578936	P04, M06, C010, C011, C013	
	*Mafa-ULBP4*3*	AB578938	M03, C007	
	*Mafa-ULBP4*4*	AB578939	M03, C006	
	*Mafa-ULBP4*5*	AB578940	P04, P05, M05, M06, C012, C013	
	*Mafa-ULBP4*6*	AB578941	M05, C010, C011	
	*Mafa-ULBP4*7.1*	AB578942	M01, C002	
	*Mafa-ULBP4*7.2*	AB578943	P03, C008	
	*Mafa-ULBP4*8*	AB578944	P03, M04, C008, C009	
	*Mafa-ULBP4*9*	AB578945	P01, C001, C002	
	*Mafa-ULBP4*10*	AB578946	M04, C009	
	*Mafa-ULBP4*11*	AB578947	P02, C007	
	*Mafa-ULBP4*12*	AB578948	M02, C005	

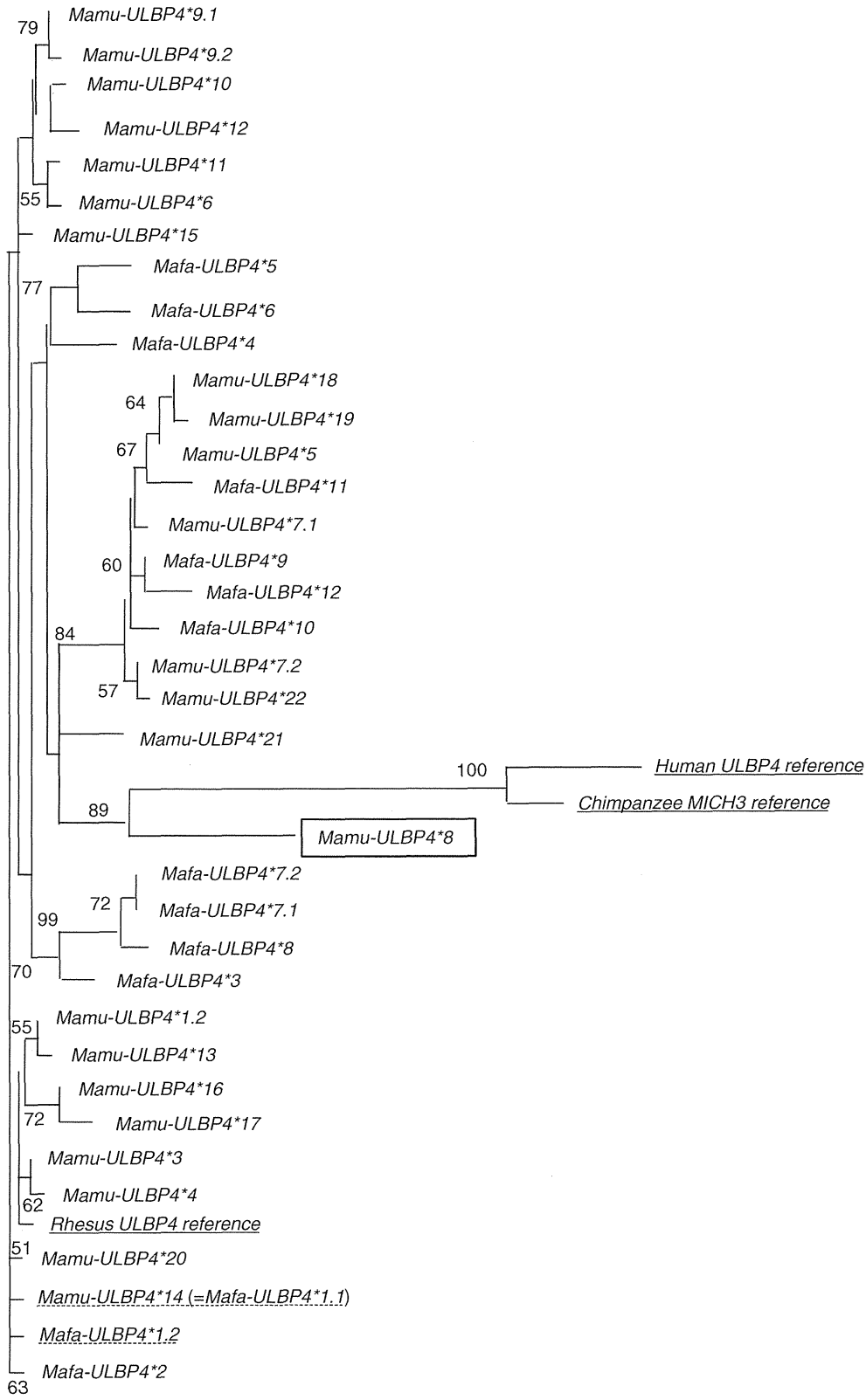

Fig. 1 Phylogenetic tree of *Mamu-* and *Mafa-ULBP4/RAET1E* alleles. A phylogenetic tree of *ULBP4/RAET1E* sequences spanning from exons 2 to 3, obtained in this study, was constructed by using the neighbor-joining method with bootstrap values of 5,000 replications. Values are indicated as percentages, and only those with more than 50% are shown. Sequences of human *ULBP4/RAET1E* (AY252119), chimpanzee *MICH3* (AY032638), and rhesus *ULBP4/RAET1E* (NC007861) were *underlined* and included in the analysis as reference sequences. Alleles represented with *broken underlines* had identical amino acid sequences predicted from the nucleotide sequences. The allele containing an in-frame termination codon was *boxed*

Results

ULBP4/RAET1E polymorphisms in the rhesus macaque

In the rhesus macaque genome (Gibbs et al. 2007), there are two paralogous genes for *ULBP4/RAET1E*, one of which appears to be functional, whereas the other is a pseudogene because it contains a large deletion containing the most part of exons 2, 3, and 4. Therefore, we designed primer pairs to amplify the region containing exons 2 and 3, which encode for α1 and α2 domains of ULBP4/RAET1E molecule, respectively, from the functional *ULBP4/RAET1E*. By using the primer pair, we obtained *ULBP4/RAET1E* sequences from 38 individuals of rhesus macaque. Because one or two sequences were obtained from each individual, the sequences were considered to be alleles of *ULBP4/RAET1E*. They were classified into 25 different alleles, designated as *Mamu-ULBP4*1.1* to *Mamu-ULBP4*22*, submitted to DDBJ, and given accession numbers (Table 1). The allele names with different numbers indicate that they are different in predicted amino acid sequences, whereas the alleles with the same deduced amino acid sequences but different nucleotide sequences, such as *Mamu-ULBP4*1.1* and *Mamu-ULBP4*1.2*, are designated as subtypes. None of the sequences obtained in this study was identical to the reference sequence, NC007861, which was previously deposited to the GenBank database as the rhesus *ULBP4/RAET1E*. On the other hand, when the sequences were aligned referring the human *ULBP4/RAET1E*, one rhesus allele (*Mamu-ULBP4*8*) was found to contain a nonsense mutation at codon 29, which would make the ULBP4/RAET1E molecule non-functional.

ULBP4/RAET1E polymorphisms in the crab-eating macaque

By using the primer pair designed for the rhesus *ULBP4/RAET1E*, we could amplify the *ULBP4/RAET1E* sequences from 24 individuals of the crab-eating macaque. Sequencing analysis revealed 14 different *ULBP4/RAET1E* alleles, and inheritance of each allele was confirmed by family studies. The identified allele sequences were submitted to DDBJ, given accession numbers, and designated as *Mafa-ULBP4*1.1* to *Mafa-ULBP4*12* (Table 1). The nucleotide sequences from exons 2 to 3 of *Mamu-ULBP4*14* were identical to those of *Mafa-ULBP4*1.1* and differed by only one nucleotide in intron 2 from those of *Mafa-ULBP4*1.2*. In addition, a neighbor-joining analysis performed by using nucleotide sequences spanning from exons 2 to 3 showed that the alleles of rhesus and crab-eating macaques were not separately clustered from each other (Fig. 1).

Comparative analysis of *ULBP4/RAET1E*

The alignment of *ULBP4/RAET1E* sequences from rhesus and crab-eating macaques with those from humans and chimpanzees showed that the macaque genes were homologous to the human gene by more than 90% and were equally diverged (Fig. 2). In addition, rhesus and crab-

```
                                                                                50
                Human :GHSLCFNFTI KSLSRPGQPW CEAQVFLNKN LFLQYNSDNN MVKPLGLLGK KVYATSTwge
            Chimpanzee :---------- -L-------- ---------- ---------- ---------- --N-------
        Rhesus macaque :A--------- --W------- ------M-K- -----D—S- ---------- --N-----Q-
    Crab-eating macaque :A--------- --W------- ------M--- -F---D—SN ---------- --N-----Q-

                                                                    100
                Human :ltqtlgevgr dlrmllcdIK PQIKTSDPST LQVEMFCQRE AERCTGASWQ FATNGEKSLL
            Chimpanzee :---M------ ------L--- ------G--- ---------- ---------- --I-------
        Rhesus macaque :---K------ ------L-V- ------GP-- -----L---- ---------- -TI----C--
    Crab-eating macaque :---------- -LM---L-V- P-----G--- L----L---- ---------- -TI----C--

                                                        150
                Human :FDAMNMTWTV INHEAskike twkkdrglek yfrklskgdc dhwlreflgh weampEPTV
            Chimpanzee :---------- ---------- ---------- ---------- ---------- --------Q
        Rhesus macaque :F----M---- ----AS---- ---K------ ------M--- N------L-- Q-A-----Q
    Crab-eating macaque :---------- -----S---- ---------- ------M--- N-WLR----- Q------TQ
```

Fig. 2 Alignment of deduced amino acid sequences of α1 and α2 domains of ULBP4/RAET1E. Amino acid sequences were deduced from the nucleotide sequences of *ULBP4/RAET1E* or *MICH3* from humans (AY252119), chimpanzees (AY032638), rhesus macaques (NC007861), and crab-eating macaques (AY032639). *Numbers* above the sequences represent the amino acid positions in mature protein. *Dashes* indicate identical sequences. Sequences for the predicted α helix structure were indicated by *small italicized characters*. Positions of polymorphic sites in the *human*, *rhesus macaque*, and *crab-eating macaque* were *underlined*

Table 2 Single nucleotide polymorphisms of ULBP4 gene among human and Old World monkeys

	Number of alleles	Exon 2		Intron 2	Exon 3	
		Polymorphism	Non-synonymous change (%)	Polymorphism	Polymorphism	Non-synonymous change (%)
Human	5	2	2 (100%)	3	3	3 (100%)
Rhesus macaque	25	9	5 (55.6%)	22	22	14 (63.6%)
Crab-eating macaque	14	17	9 (52.9%)	18	16	9 (56.3%)

eating macaques showed a higher degree of polymorphism in the analyzed region, namely, exon 2, intron 2, and exon 3, than in humans (Table 2). All polymorphisms found in exons of human *ULBP4/RAET1E* were non-synonymous, whereas a considerable part of the polymorphisms were synonymous in the Old World monkeys. On the other hand, the polymorphic sites in the rhesus macaque (positions 29, 46, 59, 64, 79, 88, 112, 121, 126, 135, 136, 144, 157, 158, 161, 168, 171, and 173) and the crab-eating macaque (positions 32, 39, 40, 59, 72, 73, 79, 91, 112, 136, 163, 164, 165, 171, 178, and 179) were shared at five positions (59, 79, 112, 136, and 171) by each other, whereas only one position (position 112) was shared with polymorphic sites in humans (positions 53, 99, 112, and 113) (Fig. 2). In addition, a termination at position 29 was found in a rhesus macaque allele *Mamu-ULBP4*8*; a single amino acid deletion caused by deletions of a total of three nucleotides was found in a crab-eating macaque allele *Mafa-ULBP4*6* [i.e., TGGCTCAGG sequences corresponding to codons 163–165 were changed to TGCTCA, which may be due to two different deletions at codons 163 (from TGG to TG) and 165 (from AGG to A)], whereas such polymorphisms were not observed in humans. These findings suggest that a selection pressure to generate and maintain the polymorphic sites might be considerably different between the lineages of humans and the Old World monkeys.

Discussion

It has been suggested that the ancestral gene for the ULBP/REAT molecule of placental mammals was originally diverged and duplicated in each species after an emigration from the MHC region (Kondo et al. 2010). In humans, MHC genes (*HLA* genes) are clustered and mapped on the short arm of chromosome 6, 6p21.3, whereas the *ULBP/RAET1* genes are located on the long arm of chromosome 6, 6q25.1. As for the *MHC* genes in the macaque, it was previously reported that rhesus macaque MHC, e.g., BAT1 gene, was localized to chromosome 6q24 by using fiber-fluorescence in situ hybridization (Huber et al. 2003) and cynomolgus (crab-eating) macaque MHC, e.g., Mafa-A and Mafa-B genes, was cytogenetically mapped to chromosome 6p13 (Liu et al. 2007), although the rhesus macaque MHC is mapped on the short arm of chromosome 4 in the draft genome sequence database of rhesus macaques (Gibbs et al. 2007); e.g., Mamu-A and BAT1 were mapped from positions 29, 517, 308 to 29, 520, 221 and from 31, 164, 822 to 31, 175, 032, respectively, on chromosome 4 (data were obtained from the UCSC Genome Browser at http://genome.ucsc.edu/cgi-bin/hgGateway). The discrepancy between the cytogenetic mapping and the assignment in draft genome sequence should be resolved in the future. On the other hand, it is interesting to note that each member of the *ULBP/RAET1* gene family, except for *ULBP6*, is completely or partially duplicated in the rhesus genome. As for the *ULBP4/RAET1E*, two related sequences, LOC695031 (NC007861) and LOC694265, have been identified as orthologs of human *ULBP4/RAET1E*. On the other hand, the configuration of *ULBP/RAET1* loci in the crab-eating macaque genome remained unknown. Because LOC694265 was a pseudogene lacking most part of the coding exons, we designed PCR primers by referring the NC007861 sequence. By using the designed primers, we could successfully amplify *ULBP4/RAET1E* alleles from both rhesus and crab-eating macaques.

In this study, we identified a total of 25 and 14 alleles from rhesus and crab-eating macaques, respectively. One of the rhesus macaque alleles had identical sequences to one of the crab-eating macaque alleles, and the phylogenetic analysis demonstrated that the *ULBP4/RAET1E* alleles were widely diverged. None of the alleles identified in this study were identical to the previously reported sequence NC007861, which was derived from an individual of Indian rhesus macaque. Given that we analyzed rhesus macaques of Burmese origin in this study, and allele distribution of MHC-related polymorphic genes are well known to be largely dependent on the habitat regions, the extent of diversity and variation in *ULBP4/RAET1E* may be further expanded.

It was demonstrated that the diversity of *ULBP4/RAET1E* in the Old World monkeys was much higher than that of human *ULBP4/RAET1E*. It is possible that the genes in the *ULBP/RAET1* locus, in particular, *ULBP4/RAET1E* and *ULBP/RAET1*s, might be highly polymorphic in the

Old World monkeys. We therefore investigated ten unrelated rhesus macaque subjects, in which we had detected 16 *ULBP4/RAET1E* alleles for polymorphisms in the adjacent *ULBP/RAET1* genes. We found one *ULBP1/RAET1I* allele, seven *ULBP2/RAET1H* alleles, and one *ULBP3/RAET1N* allele in these subjects. The observation suggested that *ULBP4/RAET1E* was highly polymorphic as compared to the adjacent *ULBP/RAET1* genes.

We revealed a high degree of polymorphism in the *ULBP4/RAET1E* of the rhesus and crab-eating macaques, although about half of the polymorphisms were synonymous changes (Table 2). Albeit the expression of the ULBP4/RAET1E molecule is known to be involved in the recognition of tumor cells by the NKG2D receptor (Cao et al. 2008; Kong et al. 2009), the functional significance of the polymorphisms in the extracellular domain of the ULBP4/RAET1E molecules remained unknown. To investigate a possible role of the polymorphisms, we have created a 3-D structure model of rhesus ULBP4/RAET1E molecule by using the structure data of human ULBP3/RAET1N in complex with NKG2D (Radaev et al. 2001) as the reference. As shown in Fig. 3, only one polymorphic site at 173 was on the surface of the α helix pointing to the NKG2D receptor, five sites at 59, 136, 144, 161, and 165 were positioned outside the α helix, and only two sites at 32 and 91 were mapped on the β sheet in the groove. The other polymorphic sites were on the β sheet outside of the groove or were not on the surface of the α helix. In addition, expression of *ULBP4/RAET1E* is predominantly found in the skin and tumor tissues and not induced by viral infection in normal cells (Chalupny et al. 2003; Eagle et al. 2006). These observations suggest that the polymorphisms are unlikely to be involved in the differential presentation of characteristic small molecules bound by the ULBP4/RAET1E molecules, as found in the presentation of antigenic peptides by the MHC molecules. Nevertheless, highly prevalent polymorphisms leading to amino acid replacements suggest that a selection pressure had operated on the configuration of diversity in *ULBP4/RAET1E*.

Of particular interest in this study was the rhesus macaque allele *Mamu-ULBP4*8*, which was supposed to contain a stop codon in the exon 2 coding sequence that would truncate the most part of the molecule. This is the first report of a non-functional *ULBP/RAET1* allele in primates; however, a similar situation was reported for another NKG2D ligand gene, *MIC*. For example, a specific human *MIC* haplotype linked to HLA-B*048 consists of non-functional *MIC* genes, in which *MICA* was deleted and *MICB* contained a termination codon (Ota et al. 2000); the non-functional *MIC* haplotype is widely distributed in the East Asian populations (Komatsu-Wakui et al. 2001). It is interesting to note that there are two distinct and polymorphic genes for *MIC* in the rhesus macaque, *MICA* (previously designated as *MIC1* and *MIC3*) and *MICB* (previous *MIC2*); however, they are not considered to be orthologous to the human *MICA* and *MICB* genes, respectively (Seo et al. 1999, 2001; Doxiadis et al. 2007; Averdam et al. 2007). Because members of the MIC and ULBP/RAET1 molecules are structurally related (Li et al. 2002), there is a functional redundancy in the recognition by NKG2D, and thus, the presence of a null allele had been allowed during the evolution of primates.

In the present study, we demonstrated the *ULBP4/RAET1E* allelic polymorphisms not only in the rhesus macaque but also in the crab-eating macaque. Although the localization of *ULBP4/RAET1E* in the crab-eating macaque

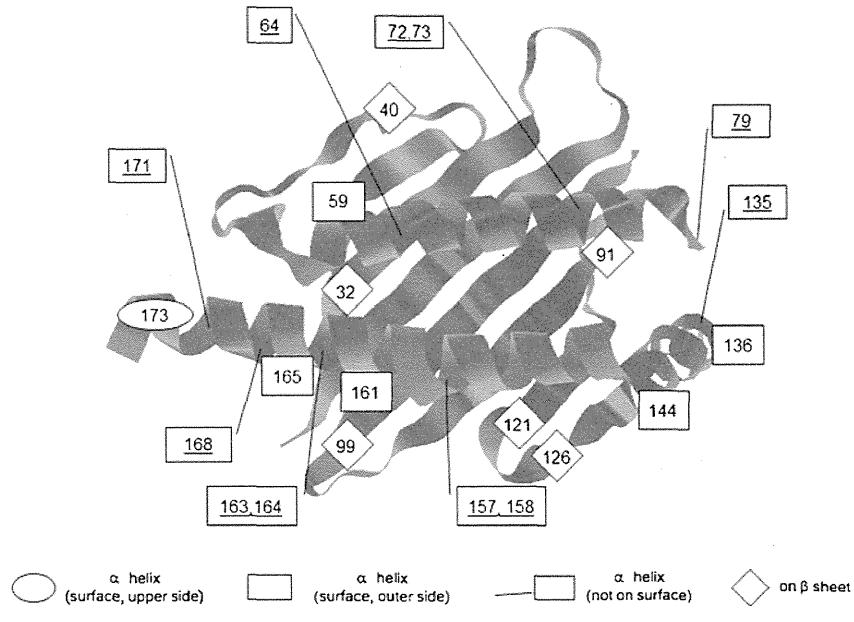

Fig. 3 Mapping of polymorphic sites on the structure model of the macaque ULBP4/RAET1E molecule. Polymorphic sites found in the Old World monkeys were mapped on the 3-D structure model of ULBP4/RAET1E. Residues on the upper and outer sides of the α helix structure were indicated by a *circle* and *squares*, respectively. Residues not found on the surface of the α helix were *underlined*, and those on the β sheet structure were represented by *rhombi*

genome is unknown, a homology search showed that a *Mafa-MICH3* gene (AY032639) was homologous to *Mafa-ULBP4/RAET1E* because the nucleotide sequences of *Mafa-ULBP4*1.1* showed a 96% homology to *Mafa-MICH3*. Similarly, nucleotide sequences of a chimpanzee gene, *Patr-MICH3* (AY032638), showed a 94% homology to the rhesus *ULBP4/RAET1E*. These findings strongly suggest that *MICH3* in the crab-eating macaque and chimpanzee is orthologous to *ULBP4/RAET1E* in the human and rhesus macaque.

In conclusion, we revealed a large diversity of *ULBP4/RAET1E* in two related species of the Old World monkey. Because there were extremely large polymorphisms in the extracellular domain of the ULBP4/RAET1E molecule in the Old World monkey, which was larger than that in the human, the functional impact of the polymorphisms and its significance in the evolution of primates should be investigated in future studies.

Acknowledgments We thank Ms. Yukiko Ueda for her technical assistance. This work was supported, in part, by research grants from the Ministry of Health, Labor and Welfare, Japan; the Japan Health Science Foundation; the program of Founding Research Centers for Emerging and Reemerging Infection Disease; the program of Research on Publicly Essential Drugs and Medical Devices; grants-in-aid for scientific research from the Ministry of Education, Culture, Sports, Science, and Technology (MEXT), Japan; a support for women researchers from the Tokyo Medical and Dental University; and a grant from the Life Science Institute Foundation.

References

Antoun A, Jobson S, Cook M, O'Callaghan CA, Moss P, Briggs DC (2010) Single nucleotide polymorphism analysis of the NKG2D ligand cluster on the long arm of chromosome 6: extensive polymorphisms and evidence of diversity between human populations. Hum Immunol 71:610–620

Averdam A, Seelke S, Grützner I, Ronser C, Roos C, Westphal N, Stahl-Hennig C, Muppala V, Schrod A, Sauermann U, Dressel R, Walter L (2007) Genotyping and segregation analyses indicate the presence of only two functional MIC genes in rhesus macaques. Immunogenetics 59:247–251

Bacon L, Eagle RA, Meyer M, Easom N, Young NT, Trowsdale J (2004) Two human ULBP/RAET1 molecules with transmembrane region are ligands for NKG2D. J Immunol 173:1078–1084

Bauer S, Groh V, Wu J, Steinle A, Phillips JH, Lanier LL, Spies T (1999) Activation of NK cells and T cells by NKG2D, a receptor for stress-inducible MICA. Science 285:727–729

Cao W, Xi X, Wang Z, Dong L, Hao Z, Cui L, Ma C, He W (2008) Four novel ULBP splice variants are ligands for human NKG2D. Int Immunol 20:981–991

Chalupny NJ, Sutherland CL, Lawrence WA, Rein-Weston A, Cosman D (2003) ULBP4 is a novel ligand for human NKG2D. Biochem Biophys Res Commun 305:129–135

Cosman D, Müllberg J, Sutherland CL, Chin W, Armitage R, Fanslow R, Kubin M, Chalupny NJ (2001) ULBPs, novel MHC class I–related molecules, bind to CMV glycoprotein UL16 and stimulate NK cytotoxicity through the NKG2D receptor. Immunity 14:123–133

Doxiadis GGM, Heijmans CM, Otting N, Bontrop RE (2007) MIC gene polymorphism and haplotype diversity in rhesus macaques. Tissue Antigens 69:212–219

Eagle RA, Traherne JA, Ashiru O, Wills MR, Trowsdale J (2006) Regulation of NKG2D ligand gene expression. Hum Immunol 67:1159–1169

Eagle RA, Flack G, Warford A, Martinez-Borra J, Jafferji I, Traherne JA, Ohashi M, Boyle LH, Barrow AD, Caillat-Zucman S, Young NT, Trowsdale J (2009a) Celllar expression, trafficking, and function of two isoforms of human ULBP5/RAET1G. Pros ONE 4:e4503

Eagle RA, Traherne JA, Hair JR, Jafferji I, Trowsdale J (2009b) ULBP6/RAET1L is an additional human NKG2D ligand. Eur J Immunol 39:3207–3216

Gibbs RA, Rogers J, Katze MG et al (2007) Evolutionary and biomedical insights from the rhesus macaque genome. Science 316:222–234

Huber I, Walter L, Wimmer R, Pasantes JJ, Günther E, Schempp W (2003) Cytogenetic mapping and orientation of the rhesus macaque MHC. Cytogenet Genome Res 103:144–1449

Komatsu-Wakui M, Tokunaga K, Ishikawa Y, Leelayuwat C, Kashiwase K, Tanaka H, Moriyama S, Nakajima F, Park MH, Jia GJ, Chimge NO, Sideltseva EW, Juji T (2001) Wide distribution of the MICA-MICB null haplotype in East Asians. Tissue Antigens 57:1–8

Kondo M, Maruoka T, Otsuka N, Kasamatsu J, Fugo K, Hanzawa N, Kasahara M (2010) Comparative genomic analysis of mammalian NKG2D ligand family genes provides insights into their origin and evolution. Immunogenetics 62:441–450

Kong Y, Cao W, Xi X, Ma C, Cui L, He W (2009) The NKG2D ligand ULBP4 binds to TCRgamma9/delta2 and induces cytotoxicity to tumor cells through both TCRgammadelta and NKG2D. Blood 114:310–317

Kulski JK, Anzai T, Shiina T, Inoko H (2004) Rhesus macaque class I duplicon structures, organization, and evolution within the alpha block of the major histocompatibility complex. Mol Biol Evol 21:2079–2091

Li P, McDermott G, Strong RK (2002) Crystal structures of RAE-1β and its complex with the activating immunoreceptor NKG2D. Immunity 16:77–86

Liu QY, Wang XX, Zhang JZ, Chen WH, He XW, Lin Y, Wang JF, Zhu Y, Hu SN, Wang XN (2007) Mapping cynomolgus monkey MHC class I district on chromosome 6p13 using pooled cDNAs. Biotech Histochem 82:267–272

Naruse KT, Chen Z, Yanagida R, Yamashita T, Saito Y, Mori K, Akari H, Yasutomi Y, Miyazawa M, Matano T, Kimura A (2010) Diversity of MHC class I genes in Burmese-origin rhesus macaque. Immunogenetics 62:601–611

Ota M, Bahram S, Katsuyama Y, Saito S, Nose Y, Sada M, Ando H, Inoko H (2000) On the MICA deleted-MICB null, HLA-B*4801 haplotype. Tissue Antigens 56:268–271

Otting N, Otting N, deVos-Rouweler AJM, Heijmans CMC, de Groot NG, Doxiadis GGM, Bontrop RE (2007) MHC class I A region diversity and polymorphism in macaque species. Immunogenetics 59:367–375

Pappworth IY, Wang EC, Rowe M (2007) The switch from latent to productive infection in Epstein-Barr virus-infected B cell is associated with sensitization to NK cell killing. J Virol 1:474–482

Pende D, Rivera P, Marcenaro S, Chang CC, Biassoni R, Conte R, Kubin M, Cosman D, Ferrone S, Moretta L, Moretta A (2002) Major histocompatibility complex class I-related chain A and UL16-binding protein expression on tumor cell lines of different histotypes: analysis of tumor susceptibility to NKG2D-dependent natural killer cell cytotoxicity. Cancer Res 62:6178–6186

Radaev S, Rostro B, Brooks AG, Colonna M, Sun PD (2001) Conformational plasticity revealed by the cocrystal structure of NKG2D and its class I MHC-like ligand ULBP3. Immunity 5:1039–1049

Radosavljevic M, Cuillerier B, Wilson MJ, Clement O, Wicker S, Gilfillan S, Beck S, Trowsdale J, Bahram S (2001) A cluster of ten novel MHC class I related genes on human chromosome 6q24.2-q25.3. Genomics 79:114–123

Raulet DH (2003) Roles of the NKG2D immunoreceptor and its ligands. Nat Rev Immunol 3:781–790

Romphruk AV, Romphruk A, Naruse TK, Raroengjai S, Puapairoj C, Inoko H, Leelayuwat C (2009) Polymorphisms of NKG2D ligands: diverse RAET1/ULBP genes in northeastern Thais. Immunogenetics 61:611–617

Seo JW, Bontrop R, Walter L, Günther E (1999) Major histocompatibility complex-linked MIC genes in rhesus macaques and other primates. Immunogenetics 50:358–362

Seo JW, Walter L, Günther E (2001) Genomic analysis of MIC genes in rhesus macaques. Tissue Antigens 58:159–165

Ward J, Bonaparte M, Sacks J, Guterman J, Fogli M, Mavilio D, Barker E (2007) HIV modulates the expression of ligands important in triggering natural killer cell cytotoxic responses on infected primary T-cell blasts. Blood 110:1207–1214

Wu J, Song Y, Bakker ABH, Bauer S, Spies T, Lanier LL, Phillips JH (1999) An activating immune receptor complex formed by NKG2D and DAP 10. Science 285:730–732

Microbiology and Immunology

Microbiol Immunol 2011; **55**: 768–773
doi:10.1111/j.1348-0421.2011.00384.x

ORIGINAL ARTICLE

Major histocompatibility complex class I-restricted cytotoxic T lymphocyte responses during primary simian immunodeficiency virus infection in Burmese rhesus macaques

Midori Nakamura[1,2], Yusuke Takahara[1,2], Hiroshi Ishii[1,2], Hiromi Sakawaki[3], Mariko Horiike[3], Tomoyuki Miura[3], Tatsuhiko Igarashi[3], Taeko K. Naruse[4], Akinori Kimura[4], Tetsuro Matano[1,2] and Saori Matsuoka[2]

[1]Division for AIDS Vaccine Development, Institute of Medical Science, University of Tokyo, 4-6-1 Shirokanedai, Minato-ku, Tokyo 108-8639, [2]AIDS Research Center, National Institute of Infectious Diseases, 1-23-1 Toyama, Shinjuku-ku, Tokyo 162-8640, [3]Institute for Virus Research, Kyoto University, 53 Kawahara-cho, Shogoin, Sakyo-ku, Kyoto 606-8507, and [4]Department of Molecular Pathogenesis, Medical Research Institute, Tokyo Medical and Dental University, 2-3-10 Kandasurugadai, Chiyoda-ku, Tokyo 101-0062, Japan

ABSTRACT

Major histocompatibility complex class I (MHC-I)-restricted CD8$^+$ cytotoxic T lymphocyte (CTL) responses are crucial for the control of human immunodeficiency virus (HIV) and simian immunodeficiency virus (SIV) replication. In particular, Gag-specific CTL responses have been shown to exert strong suppressive pressure on HIV/SIV replication. Additionally, association of Vif-specific CTL frequencies with *in vitro* anti-SIV efficacy has been suggested recently. Host MHC-I genotypes could affect the immunodominance patterns of these potent CTL responses. Here, Gag- and Vif-specific CTL responses during primary SIVmac239 infection were examined in three groups of Burmese rhesus macaques, each group having a different MHC-I haplotype. The first group of four macaques, which possessed the MHC-I haplotype *90-010-Ie*, did not show Gag- or Vif-specific CTL responses. However, Nef-specific CTL responses were elicited, suggesting that primary SIV infection does not induce predominant CTL responses specific for Gag/Vif epitopes restricted by *90-010-Ie*-derived MHC-I molecules. In contrast, Gag- and Vif-specific CTL responses were induced in the second group of two *89-075-Iw*-positive animals and the third group of two *91-010-Is*-positive animals. Considering the potential of prophylactic vaccination to affect CTL immunodominance post-viral exposure, these groups of macaques would be useful for evaluation of vaccine antigen-specific CTL efficacy against SIV infection.

Key words cytotoxic T lymphocyte, human immunodeficiency virus, major histocompatibility complex, simian immunodeficiency virus.

Virus-specific CD8$^+$ CTL responses are crucial for the control of HIV and SIV replication (1–5). CTLs recognize specific epitopes which are presented on the target cell surface by binding to the MHC-I molecule. There have been many reports indicating association of MHC-I (HLA class I) genotypes with rapid or delayed AIDS progression in HIV-infected people (6–8). For instance, most of the HIV-infected individuals possessing *HLA-B*57* have a better prognosis and smaller viral loads, implicating HLA-B*57-restricted epitope-specific CTL responses in control

Correspondence
Saori Matsuoka, AIDS Research Center, National Institute of Infectious Diseases, 1-23-1 Toyama, Shinjuku-ku, Tokyo 162-8640, Japan.
Tel: 81 3 5285 1111; Fax: 81 3 5285 1165; e-mail: s-matsu@nih.go.jp

Received 11 May 2011; revised 18 July 2011; accepted 21 August 2011.

List of Abbreviations: CTL, cytotoxic T lymphocyte; HIV, human immunodeficiency virus; HLA, human leukocyte antigen; IFN-γ , gamma interferon; MHC-1, major histocompatibility complex class I; PBMC, peripheral blood mononuclear cell; SIV, simian immunodeficiency virus.

of this virus (9, 10). Indian rhesus macaques possessing the MHC-I allele Mamu-B*17 tend to show smaller viral loads after SIVmac239 challenge (11). These findings imply possible HIV control by induction of particular effective CTL responses.

The potential of Gag-specific CTL responses to contribute to viral control was suggested by a cohort study indicating association of HIV control with the breadth of Gag-specific CTL responses (12). This was supported by an *in vitro* study indicating the ability of Gag-specific CTLs to respond rapidly to SIV infection (13). We previously developed a prophylactic AIDS vaccine using a Sendai virus vector expressing SIVmac239 Gag (14) and showed that Gag-specific CTL responses were responsible for vaccine-based SIV containment in a group of Burmese rhesus macaques possessing the MHC-I haplotype *90–120-Ia* (15, 16). Furthermore, our recent study analyzing the potential of $CD8^+$ cells to suppress SIV replication *in vitro* suggested association of *in vitro* anti-SIV efficacy with numbers of Vif-specific CTL frequencies (17). We also found weaker correlation between anti-SIV efficacy and numbers of Nef-specific CTL frequencies. These results imply the potency of Gag- and Vif-specific (and possibly Nef-specific) CTLs in suppressing HIV/SIV replication.

The immunodominance patterns of these potent CTL responses could be affected by host MHC-I genotypes (18, 19). Better understanding of these MHC-I-associated CTL immunodominance patterns during primary HIV/SIV infection would contribute to elucidation of the interaction between viral replication and host CTL responses. In the present study, we examined whether Gag- and Vif-specific CTL responses are efficiently induced during primary SIVmac239 infection in three groups of Burmese rhesus macaques possessing different MHC-I haplotypes. One group did not induce Gag- or Vif-specific CTL responses, whereas the other two groups elicited Gag- and Vif-specific CTL responses efficiently. These groups of macaques would be useful for analysis of the impact of Gag- and Vif-specific CTL responses on SIV replication *in vivo*.

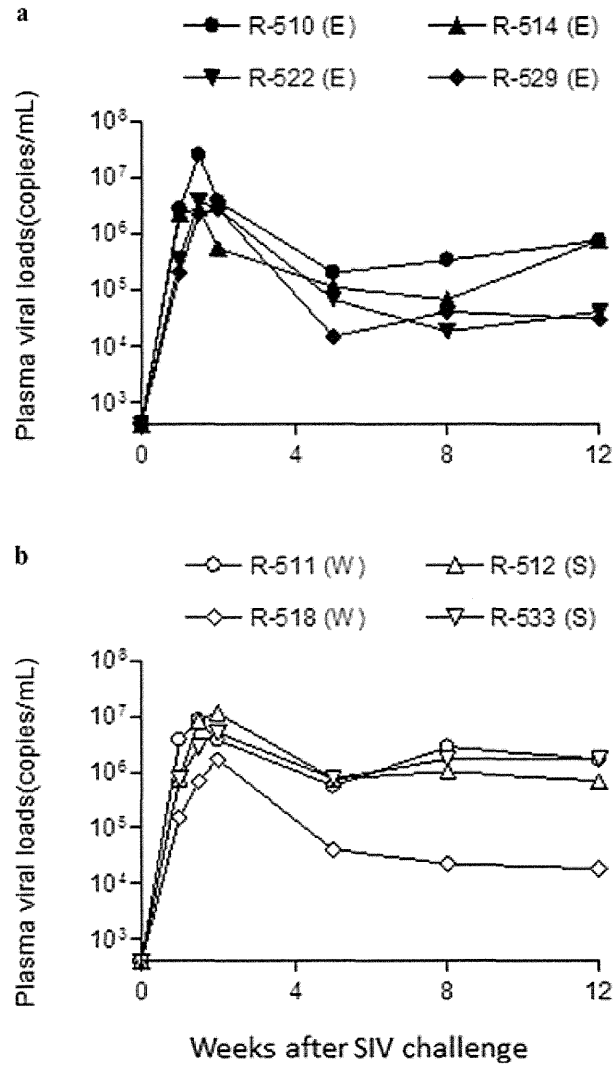

Fig. 1. Plasma viral loads after SIV challenge. (a) The first group of Burmese rhesus macaques, which possessed MHC-I haplotype *90-010-Ie* (R-510, R-514, R-522, and R-529) and (b) the second group, which possessed *89-075-Iw* (R-511 and R-518) and the third group, which possessed *91-010-Is* (R-512 and R-533) were challenged with SIVmac239. The viral loads (SIV gag RNA copies/mL) were determined as described previously (15).

MATERIALS AND METHODS

Animal experiments

Animal experiments using Burmese rhesus macaques (*Macaca mulatta*) possessing either the MHC-I haplotypes *90-010-Ie*, *89-075-Iw* or *91-010-Is* were performed in the Institute for Virus Research, Kyoto University, in accordance with the institutional regulations approved by the Committee for Experimental Use of Non-human Primates. The MHC-I haplotypes of macaques were determined as described previously (20, 21). These animals were challenged intravenously with 1000 50% tissue culture infective doses ($TCID_{50}$) of SIVmac239 (22).

Analysis of virus-specific cytotoxic T lymphocyte responses

Virus-specific $CD8^+$ T-cell frequencies were measured by flow cytometric analysis of IFN-γ induction after specific stimulation as described previously (17). PBMCs were cocultured with autologous herpesvirus papio-immortalized B-lymphoblastoid cell lines pulsed with peptide pools using panels of overlapping peptides

spanning the entire SIVmac239 Gag, Pol, Vif, Vpx, Vpr, Tat, Rev, Nef, and Env amino acid sequences. Intracellular IFN-γ staining was performed with a Cytofix-Cytoperm kit (Becton Dickinson, Tokyo, Japan) and fluorescein isothiocyanate-conjugated anti-human CD4 (Becton Dickinson), peridinin chlorophyll protein-conjugated anti-human CD8 (Becton Dickinson), allophycocyanin-conjugated anti-human CD3 (Becton Dickinson), and phycoerythrin-conjugated anti-human IFN-γ monoclonal antibodies (BioLegend, Tokyo, Japan). Specific $CD8^+$ T-cell frequencies were calculated by subtracting nonspecific IFN-γ^+ $CD8^+$ T-cell frequencies from those after peptide-specific stimulation. Specific $CD8^+$ T-cells counts of less than 100 per million PBMCs were considered negative.

RESULTS

In the present study, we used eight Burmese rhesus macaques consisting of four animals possessing MHC-I haplotype *90-010-Ie*, two possessing *89-075-Iw*, and two possessing *91-010-Is*. After a SIVmac239 challenge, all these animals failed to control viral replication and had high set-point plasma viral loads (geometric mean: 3×10^5 copies/mL) (Fig. 1).

We examined SIV-specific $CD8^+$ T cell responses at week 2 and week 6 or 12 after SIV challenge in these animals by detection of specific IFN-γ induction after stimulation using peptide mixtures (Figs. 2 and 3). At week 6 or 12, we examined $CD8^+$ T cell responses specific for the N-terminal half of Gag (Gag-N), the C-terminal half of Gag (Gag-C), Vif, Nef, the N-terminal half of Pol (Pol-N), the C-terminal half of Pol (Pol-C), Vpx, Vpr, the N-terminal half of Env (Env-N), the C-terminal half of Env (Env-C), Tat, and Rev. At week 2, however, we examined only Gag-N-, Gag-C-, Vif- and Nef-specific $CD8^+$ T cell responses because of limited availability of PBMCs.

In the first group of macaques, which possessed *90-010-Ie*, neither Gag- nor Vif-specific $CD8^+$ T cell responses were induced efficiently at week 2 (Fig. 2). Even at week 12, these responses were undetectable in most of the animals. In contrast, Nef-specific $CD8^+$ T cell responses were detected at week 2, 6, or 12 in all four animals. Env-specific $CD8^+$ T cell responses were detectable at week 12 in three of them. These results indicate that, during primary SIV infection in *90-010-Ie*-positive macaques, Gag- or Vif-specific $CD8^+$ T cell responses are not induced, however Nef-specific $CD8^+$ T cell responses are.

In the second group of macaques, which possessed *89-075-Iw*, Gag- and Vif-specific $CD8^+$ T cell responses were elicited efficiently (Fig. 3a). In the third group of macaques, which possessed *91-010-Is*, Gag-, Vif- and Nef-specific $CD8^+$ T cell responses were elicited efficiently (Fig. 3b). Other SIV antigen-specific $CD8^+$ T cell responses were not efficiently induced in these two groups except for Tat-specific $CD8^+$ T cell responses in macaque

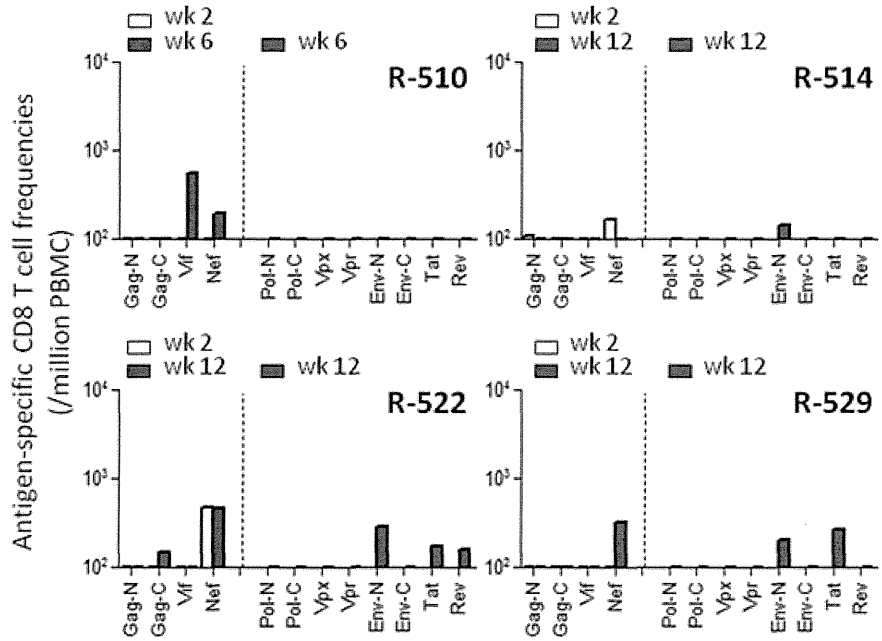

Fig. 2. SIV antigen-specific $CD8^+$ T cell frequencies in the first group of macaques, which possessed *90-010-Ie*. Gag-, Vif- and Nef-specific $CD8^+$ T cell frequencies at week 2 and Gag-, Vif-, Nef-, Pol-, Vpx-, Vpr-, Env-, Tat- and Rev-specific $CD8^+$ T cell frequencies at weeks 6 or 12 are shown.

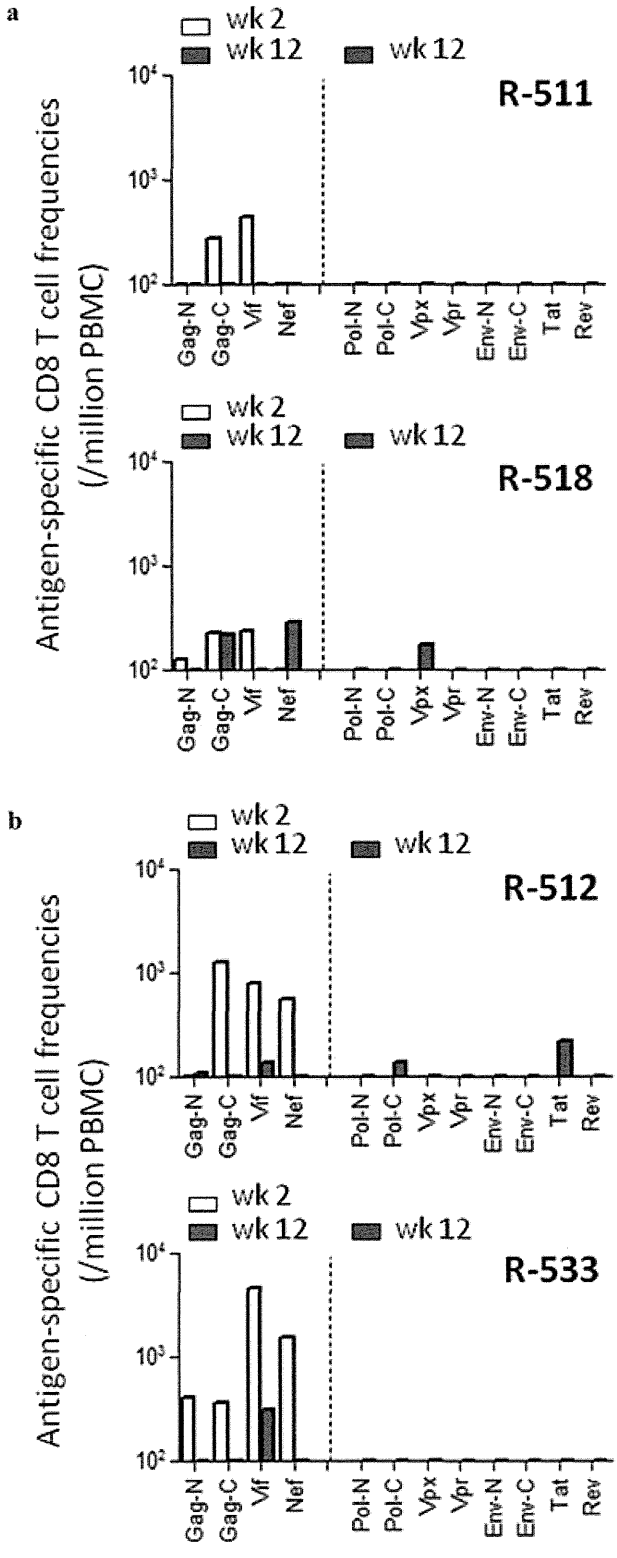

Fig. 3. SIV antigen-specific CD8$^+$ T cell frequencies in (a) the second group of macaques, which possessed *89-075-Iw* and (b) the third, which possessed *91-010-Is*.

R-512. Thus, in the four animals possessing *89-075-Iw* or *91-010-Is*, Gag- or Vif-specific CD8$^+$ T cell responses were induced more efficiently than Nef-specific ones at week 2. These responses in PBMCs were mostly diminished at week 12; possibly reflecting the considerable CTL consumption in the effector sites in animals with high viral loads.

DISCUSSION

Previous studies have indicated the potential of Gag-specific CTL responses to suppress HIV/SIV replication *in vivo* (12, 13, 16). Further, our recent study suggested the potency of Vif-specific CTL responses (17). Then, in the present study, we examined Gag- and Vif-specific CTL responses during primary SIV infection in three groups of animals, each group having a different MHC-I haplotype. Although the numbers of CTL frequencies differed between groups, the CTL responses tended have similar patterns.

Our previous study showed vaccine efficacy in a group of macaques with the MHC-I haplotype *90-120-Ia* (15, 16). Unvaccinated *90-120-Ia*-positive macaques predominantly induce Gag-specific CTL responses but fail to control viremia, while vaccinated ones show enhanced Gag-specific CTL responses and control SIV replication. $Gag_{206–216}$ epitope-specific and $Gag_{241–249}$ epitope-specific CTL responses were shown to be responsible for this vaccine-based viral control (16). However, some Gag-specific CTLs may be effective while others are not. Further analysis of this type of vaccine efficacy would contribute to understanding the requisites for vaccine-based viral control. Possibly, the *89-075-Iw*-positive or *91-010-Is*-positive animals presented in this study may be a candidate model for such analysis.

In primary SIVmac239 infection, it is speculated that some MHC-I haplotypes (referred to as type 1) are associated with Gag/Vif-specific CTL responses while others (referred to as type 2) are not. The MHC-I haplotype *90-120-Ia* described above belongs to type 1. In the present study, the second group, which possess MHC-I haplotype *89-075-Iw*, and the third, which possess *91-010-Is*, both showed efficient Gag- and Vif-specific CTL responses in primary SIV infection, although it remains undetermined whether these MHC-I haplotypes belong to type 1. In contrast, the first group of macaques, which possess MHC-I haplotype *90-010-Ie* did not show efficient Gag- or Vif-specific CTL responses in primary SIV infection. Instead, Nef-specific CTL responses were induced in all four animals. This suggests that the MHC-I haplotype *90-010-Ie* belongs to type 2; that is, primary SIV infection induces no predominant CTL responses specific for Gag/Vif epitopes

restricted by *90-010-Ie*-derived MHC-I molecules. Our results imply that CTLs exerted selective pressure on SIV *gag* and *vif* in the second/third groups but not in the first group. Larger number of animals would enable us to compare those with type 1 and 2 MHC-I haplotypes, which would contribute to our understanding of the efficacy of Gag- and Vif-specific CTL responses against SIV infection.

In developing a prophylactic CTL-inducing AIDS vaccine, it would be important to induce CTL memory resulting in potent CTL responses post-HIV exposure, while prophylactic vaccination can affect the immunodominance patterns of CTL responses post-viral exposure (23, 24). Gag- and Vif-specific CTL memory induction may be a promising vaccine strategy, but the influence of prophylactic vaccination on the patterns of CTL responses post-viral exposure would be affected by MHC-I genotypes. In the hosts in which Gag- and Vif-specific CTL responses are induced during the natural course of SIV infection, Gag- and Vif-specific CTL memory induction by prophylactic vaccination would predominantly enhance these CTL responses. In contrast, in those in whom no Gag- or Vif-specific CTL responses occurred during the natural course of SIV infection, prophylactic vaccination inducing Gag- and Vif-specific CTL responses would result in broader CTL responses. Macaques in which both MHC-I haplotypes belong to type 2 may be ideal for evaluation of this type of vaccine efficacy, but it is very difficult to accumulate those animals. It would be reasonable to use groups of macaques possessing type 2 haplotypes such as the group 1 (*90-010-Ie*-positive macaques) presented in this study for such evaluation.

In summary, by focusing on Gag- and Vif-specific CTL responses, we found two types of rhesus macaques that showed different patterns of CTL responses during primary SIV infection; one elicited Gag- and Vif-specific CTL responses but the other did not. Accumulated analyses in both types of animals would contribute to understanding the impact of these potent CTL responses on primary SIV infection.

ACKNOWLEDGMENTS

This work was supported by grants-in-aid from the Ministry of Education, Culture, Sports, Science, and Technology, grants-in-aid from the Ministry of Health, Labor, and Welfare, and a grant from Takeda Science Foundation in Japan.

REFERENCES

1. Koup R.A., Safrit J.T., Cao Y., Andrews C.A., McLeod G., Borkowsky W., Farthing C., Ho D.D. (1994) Temporal association of cellular immune responses with the initial control of viremia in primary human immunodeficiency virus type 1 syndrome. *J Virol* **68:** 4650–55.
2. Borrow P., Lewicki H., Hahn B.H., Shaw G.M., Oldstone M.B. (1994) Virus-specific CD8+ cytotoxic T-lymphocyte activity associated with control of viremia in primary human immunodeficiency virus type 1 infection. *J Virol* **68:** 6103–10.
3. Matano T., Shibata R., Siemon C., Connors M., Lane H.C., Martin M.A. (1998) Administration of an anti-CD8 monoclonal antibody interferes with the clearance of chimeric simian/human immunodeficiency virus during primary infections of rhesus macaques. *J Virol* **72:** 164–9.
4. Jin X., Bauer D.E., Tuttleton S.E., Lewin S., Gettie A., Blanchard J., Irwin C.E., Safrit J.T., Mittler J., Weinberger L., Kostrikis L.G., Zhang L., Perelson A.S., Ho D.D. (1999) Dramatic rise in plasma viremia after CD8(+) T cell depletion in simian immunodeficiency virus-infected macaques. *J Exp Med* **189:** 991–8.
5. Goulder P.J., Watkins D.I. (2004) HIV and SIV CTL escape: implications for vaccine design. *Nat Rev Immunol* **4:** 630–40.
6. Kaslow R.A., Carrington M., Apple R., Park L., Munoz A., Saah A.J., Goedert J.J., Winkler C., O'Brien S.J., Rinaldo C., Detels R., Blattner W., Phair J., Erlich H., Mann D.L. (1996) Influence of combinations of human major histocompatibility complex genes on the course of HIV-1 infection. *Nat Med* **2:** 405–11.
7. Tang J., Tang S., Lobashevsky E., Myracle A.D., Fideli U., Aldrovandi G., Allen S., Musonda R., Kaslow R.A. (2002) Favorable and unfavorable HLA class I alleles and haplotypes in Zambians predominantly infected with clade C human immunodeficiency virus type 1. *J Virol* **76:** 8276–84.
8. Goulder P.J., Watkins D.I. (2008) Impact of MHC class I diversity on immune control of immunodeficiency virus replication. *Nat Rev Immunol* **8:** 619–30.
9. Migueles S.A., Sabbaghian M.S., Shupert W.L., Bettinotti M.P., Marincola F.M., Martino L., Hallahan C.W., Selig S.M., Schwartz D., Sullivan J., Connors M. (2000) HLA B*5701 is highly associated with restriction of virus replication in a subgroup of HIV-infected long term nonprogressors. *Proc Natl Acad Sci USA* **97:** 2709–14.
10. Altfeld M., Addo M.M., Rosenberg E.S., Hecht F.M., Lee P.K., Vogel M., Yu X.G., Draenert R., Johnston M.N., Strick D., Allen T.M., Feeney M.E., Kahn J.O., Sekaly R.P., Levy J.A., Rockstroh J.K., Goulder P.J., Walker B.D. (2003) Influence of HLA-B57 on clinical presentation and viral control during acute HIV-1 infection. *AIDS* **17:** 2581–91.
11. Yant L.J., Friedrich T.C., Johnson R.C., May G.E., Maness N.J., Enz A.M., Lifson J.D., O'Connor D.H., Carrington M., Watkins D.I. (2006) The high-frequency major histocompatibility complex class I allele Mamu-B*17 is associated with control of simian immunodeficiency virus SIVmac239 replication. *J Virol* **80:** 5074–7.
12. Kiepiela P., Ngumbela K., Thobakgale C., Ramduth D., Honeyborne I., Moodley E., Reddy S., de Pierres C., Mncube Z., Mkhwanazi N., Bishop K., van der Stok M., Nair K., Khan N., Crawford H., Payne R., Leslie A., Prado J., Prendergast A., Frater J., McCarthy N., Brander C., Learn G.H., Nickle D., Rousseau C., Coovadia H., Mullins J.I., Heckerman D., Walker B.D., Goulder P. (2007) CD8+ T-cell responses to different HIV proteins have discordant associations with viral load. *Nat Med* **13:** 46–53.
13. Sacha J.B., Chung C., Rakasz E.G., Spencer S.P., Jonas A.K., Bean A.T., Lee W., Burwitz B.J., Stephany J.J., Loffredo J.T., Allison D.B., Adnan S., Hoji A., Wilson N.A., Friedrich T.C., Lifson J.D., Yang O.O., Watkins D.I. (2007) Gag-specific $CD8^+$ T lymphocytes recognize infected cells before AIDS-virus integration and viral protein expression. *J Immunol* **178:** 2746–54.
14. Matano T., Kano M., Nakamura H., Takeda A, Nagai Y. (2001) Rapid appearance of secondary immune responses and protection from acute CD4 depletion after a highly pathogenic

immunodeficiency virus challenge in macaques vaccinated with a DNA prime/Sendai virus vector boost regimen. *J Virol* **75:** 11891–6.
15. Matano T., Kobayashi M., Igarashi H., Takeda A., Nakamura H., Kano M., Sugimoto C., Mori K., Iida A., Hirata T., Hasegawa M., Yuasa T., Miyazawa M., Takahashi Y., Yasunami M., Kimura A., O'Connor D.H., Watkins D.I., Nagai Y. (2004) Cytotoxic T lymphocyte-based control of simian immunodeficiency virus replication in a preclinical AIDS vaccine trial. *J Exp Med* **199:** 1709–18.
16. Kawada M., Tsukamoto T., Yamamoto H., Iwamoto N., Kurihara K., Takeda A., Moriya C., Takeuchi H., Akari H., Matano T. (2008) Gag-specific cytotoxic T-lymphocyte-based control of primary simian immunodeficiency virus replication in a vaccine trial. *J Virol* **82:** 10199–206.
17. Iwamoto N., Tsukamoto T., Kawada M., Takeda A., Yamamoto H., Takeuchi H., Matano T. (2010) Broadening of $CD8^+$ cell responses in vaccine-based simian immunodeficiency virus controllers. *AIDS* **24:** 2777–87.
18. Loffredo J.T., Bean A.T., Beal D.R., Leon E.J., May G.E., Piaskowski S.M., Furlott J.R., Reed J., Musani S.K., Rakasz E.G., Friedrich T.C., Wilson N.A., Allison D.B., Watkins D.I. (2008) Patterns of CD8+ immunodominance may influence the ability of Mamu-B*08-positive macaques to naturally control simian immunodeficiency virus SIVmac239 replication. *J Virol* **82:** 1723–38.
19. Tenzer S., Wee E., Burgevin A., Stewart-Jones G., Friis L., Lamberth K., Chang C.H., Harndahl M., Weimershaus M., Gerstoft J., Akkad N., Klenerman P., Fugger L., Jones E.Y., McMichael A.J., Buus S., Schild H., van Endert P., Iversen A.K. (2009) Antigen processing influences HIV-specific cytotoxic T lymphocyte immunodominance. *Nat Immunol* **10:** 636–46.
20. Takahashi-Tanaka Y., Yasunami M., Naruse T., Hinohara K., Matano T., Mori K., Miysazawa M., Honda M., Yasutomi Y., Nagai Y., Kimura A. (2007) Reference strand-mediated conformation analysis (RSCA)-based typing of multiple alleles in the rhesus macaque MHC class I Mamu-A and Mamu-B loci. *Electrophoresis* **28:** 918–24.
21. Naruse T.K., Chen Z., Yanagida R., Yamashita T., Saito Y., Mori K., Akari H., Yasutomi Y., Miyazawa M., Matano T., Kimura A. (2010) Diversity of MHC class I genes in Burmese-origin rhesus macaques. *Immunogenetics* **62:** 601–11.
22. Kestler H.W. 3rd, Ringler D.J., Mori K., Panicali D.L., Sehgal P.K., Daniel M.D., Desrosiers R.C. (1991) Importance of the nef gene for maintenance of high virus loads and for development of AIDS. *Cell* **65:** 651–62.
23. Tsukamoto T., Takeda A., Yamamoto T., Yamamoto H., Kawada M., Matano, T. (2009) Impact of cytotoxic-T-lymphocyte memory induction without virus-specific CD4+ T-cell help on control of a simian immunodeficiency virus challenge in rhesus macaques. *J Virol* **83:** 9339–46.
24. Takahara Y., Matsuoka S., Kuwano T., Tsukamoto T., Yamamoto H., Ishii H., Nakasone T., Takeda A., Inoue M., Iida A., Hara H., Shu T., Hasegawa M., Sakawaki H., Horiike M., Miura T., Igarashi T., Naruse T.K., Kimura A., Matano T. (2011) Dominant induction of vaccine antigen-specific cytotoxic T lymphocyte responses after simian immunodeficiency virus challenge. *Biochem Biophys Res Commun* Epub ahead of print.

Toll-Like Receptor 2 Gene Polymorphisms Associated with Aggressive Periodontitis in Japanese

Marika Takahashi[1,2], Zhiyong Chen[2,3,5], Kaoru Watanabe[1], Hiroaki Kobayashi[1], Toshiaki Nakajima[2,4], Akinori Kimura[2,4,*] and Yuichi Izumi[1]

[1]Section of Periodontology, Department of Hard Tissue Engineering, Graduate School of Medical and Dental Science, [2]Department of Molecular Pathogenesis, Medical Research Institute, [3]Department of Vascular and Applied Surgery, Graduate School of Medical and Dental Sciences, and [4]Laboratory of Genome Diversity, Graduate School of Biomedical Science, Tokyo Medical and Dental University, [5]Department of Rheumatology and Immunology, The Affiliated Drum Tower Hospital, Nanjing University Medical School, Nanjing, China

Abstract: *Background and Objective:* Aggressive periodontitis is a rare and very severe periodontal disease of early onset, which is closely associated with *Porphyromonas.gingivalis* (*P.g.*) infection in the Japanese population. *TLR2* encodes Toll-like receptor 2, which plays an important role in the protective response to *P.g.* infection. We investigated a possible association between *TLR2* and aggressive periodontitis.

Material and Methods: Of 2,460 Japanese patients with periodontitis, 38 patients with aggressive periodontitis were enrolled in this study. These 38 aggressive periodontitis patients and 190 Japanese healthy controls were examined for an insertion/deletion (Ins/Del) polymorphism in exon 1, a polymorphism in intron 1 (rs7696323), and a synonymous polymorphism in exon 3 (rs3804100) in *TLR2*.

Results: We found significant associations of resistance to aggressive periodontitis with the Ins allele (allele frequency in the patients versus controls, 0.540 *vs.* 0.676, OR=0.56, 95% confidence interval (CI); 0.34-0.92, p=0.022) and the T allele of rs3804100 (0.579 *vs.* 0.716, OR=0.55, 95% CI; 0.33-0.91, p=0.018), although the C allele of rs7696323 showed no significant association (0.733 vs. 0.829, OR=0.58). A permutation test of Ins/Del-rs7696323-rs3804100 haplotype revealed a significant association between Ins-C-T haplotype (0.252 *vs.* 0.479, p=0.0003) and resistance to aggressive periodontitis.

Conclusions: The *TLR*2 polymorphisms were suggested to confer protection against aggressive periodontitis in a Japanese population. The association should be replicated in other cohorts to further identify the responsible *TLR* polymorphism(s) involved in the pathogenesis of aggressive periodontitis.

Keywords: TLR2, polymorphism, aggressive periodontitis, haplotype.

INTRODUCTION

Aggressive periodontitis (AgP) is a rare and severe phenotype of periodontitis characterized by rapid bone destruction and attachment loss in the absence of any systemic disease, often with familial aggregation, according to the 1999 International Classification of Periodontal Diseases criteria. The rate of AgP crisis is almost 0.03% in Japanese. Periodontitis is caused by infection with gram-negative bacteria and the subsequent inflammatory response induces destruction of periodontal tissue. Progression of AgP is so rapid that, if not treated, supporting tissues around teeth may be lost early in the life. If predisposing factors to AgP would be defined, patients carrying the predisposing factors could be treated in an early stage to prevent disease progression and to save their teeth. It is well known that susceptibility to periodontitis is influenced by both environmental (such as older age, smoking status, plaque control) and genetic factors. To reveal the genetic predisposing factors to periodontal diseases, many association studies have targeted functional polymorphisms in genes associated with inflammatory cytokines for chronic periodontitis. For example, Kornman firstly reported in 1997 that chronic periodontitis was related to interleukin (IL)-1 *(IL-1)* polymorphism [1] . Following this report, many other studies attempted to elucidate the associations of chronic periodontitis (CP) with polymorphisms in other genes, including *IL-6* and Vitamin D receptor (*VDR*) [2, 3]. These results suggested that unregulated production of inflammatory cytokines would be a risk factor for chronic periodontitis.

Association studies for AgP have also been performed for inflammatory cytokine genes, reporting that the susceptibility to AgP was associated with a *IL-13* polymorphism at -1112 in Taiwanese [4], and IL-1α (*IL-1A*) polymorphism at +4845 and IL-1β (*IL-1B*) polymorphism at -511 were asso-

*Address correspondence to this author at the Department of Molecular Pathogenesis, Medical Research Institute, Tokyo Medical and Dental University, 1-5-45 Yushima, Bunkyo-ku, Tokyo 113-8510, Japan;
Tel: +81-3-5803-4905; Fax: +81-3-5803-4907, Email: akitis@mri.tmd.ac.jp

1874-2106/11

ciated in Chinese males [5]. In addition, the association of AgP with the *IL-1* gene cluster region was investigated in an Italian population, which demonstrated a significant association with polymorphisms in the genes for IL-1 receptor antagonist (*IL1-RN*) and in *IL-1B* [6]. Furthermore, other gene polymorphisms in genes for oestrogen receptor-α (*ERA*), *VDR*, N-formylpeptide receptor (*FPR*), CC chemokine receptor 2 (*CCR2*), and monocyte chemoattractant protein I (*MCP-1*) were reported to be associated with AgP in some ethnic groups [7].

Porphyromonas gingivalis (*P.g.*) is a predominant gram-negative periodontopathic bacterium which is strongly associated with AgP in Japanese populations [8, 9], although *Aggregatibacter actinomycetemcomitans* (*A.a.*) is the strongest candidate of AgP causative bacterium in other ethnic populations [10, 11]. Component of *P.g.* is reported to be a ligand for TLR2, although *A.a.* is recognized by TLR4 [12], suggesting that TLR2 plays a key role in protective response against *P.g.* in Japanese AgP. However, there have been few studies on the relationship between AgP and polymorphisms, in the TLR genes. Although one study demonstrated a significant association between CP and a polymorphism in *TLR4* [13], another study could not replicate the significant association [3]. On the other hand, no association was observed with a *TLR2* polymorphism, Agg753Gln, in a German population [14], and a study in Japanese subjects also showed no association of CP with the *TLR2* polymorphisms, Arg677Trp and Arg753Gln [13]. TLRs are type I integral membrane glycoproteins, which play crucial roles in the innate immune system *via* recognizing molecules derived from pathogens. There are different TLR types, and different TLRs recognize a variety of pathogen-associated molecules, including lipids and nucleic acids [15]. It was reported that TLR2 is involved in the recognition of pathogenic bacteria in periodontal disease [16-18]. Although the association of AgP with *TLR2* polymorphisms accompanied by amino-acid replacement was not significant, another functional polymorphism, an Ins/Del in exon 1, which is related to the expressivity of *TLR2* [19], was not tested for the association. In this study, we investigated three tag polymorphisms of *TLR2* including the Ins/Del polymorphism in association with AgP in Japanese. We report here the association of *TLR2* with protection against AgP.

MATERIALS AND METHODS

Subjects

Two thousands and four hundreds sixty patients with periodontitis who visited Tokyo Medical and Dental University Dental Hospital from June 2009 to July 2010, were examined. All AgP cases, a total of 38 unrelated Japanese patients (21 males and 17 females; diagnosed with AgP based on the 1999 International Workshop for Classification of Periodontal Diseases and Conditions), were recruited for the study. Age at diagnosis of the patients was 34.4±6.1 years. Written informed consent was given by each patient before blood sampling. Genomic DNAs from blood were prepared by a standard method. DNA samples from 190 Japanese individuals with no systemic disease were prepared from healthy-donor derived B cell lines deposited to the Health Science Research Resource Bank, Japan Health Sciences Foundation (http://www.jhsf.or.jp/English/index_e.html). Periodontal conditions in these 190 healthy controls were unknown, although inclusion of possible AgP patients in the control would decrease the power to detect the association. The research was conducted in full accordance with ethical principles, including the World Medical Association Declaration of Helsinki (version 2002), and the study protocol was approved by the Ethics Review Committee of the Faculty of Dentistry, Tokyo Medical and Dental University, and that of the Medical Research Institute, Tokyo Medical and Dental University.

Table 1. Clinical Characteristics of AgP Patients

Clinical Parameters[#1]	
Smokers (%)	58.1
Number of teeth present (including wisdom teeth)	26.5±3.5
Mean probing pocket depth (mm)	3.8±1.0
Frequency of bleeding on probing (%)	57.9±28.7
Frequency of alveolar bone loss (%)	41.0±23.0
Rate of probing pocket depth >4 mm (%)	76.0±22.6
Rate of probing pocket depth >7 mm (%)	37.0±22.3

[#1]Value was represented as mean ± standard deviation, when it was appropriate.

Clinical Information

Periodontal parameters and radiographs of all AgP patients were assessed at their first visit. Probing pocket depth (PPD) was measured at 6 sites per tooth. Bleeding on probing (BOP) was also recorded at 6 sites per tooth. Alveolar bone loss (BL) was investigated at two sites per tooth on the radiographs. The data for frequency of BOP, rate of PPD over 4 mm, rate of PPD over 7 mm, and frequency of alveolar bone loss are summarized in Table **1**.

Genotyping of *TLR2*

Human *TLR2* is located on chromosome 4q32 and is composed of three exons. Two tag single nucleotide polymorphism (SNP), rs7696323 in intron 1 and rs3804100 in exon 3, were selected from the International HapMap project database (HapMap Data Phase III/Rel#2, Feb09, on NCBI B36 assembly, dbSNP b126) by cut-off criteria of minor allele frequency >0.1 and r square <0.8 in the Japanese population. In addition, an insertion/deletion (Ins/Del) polymorphism at -196 to -174 was investigated. The restriction fragment length polymorphism method was used for the genotyping of rs7696323 and rs3804100. Briefly, polymerase chain reaction (PCR) was performed with primer pairs, 5'-ggcccctagctcctgtcc-3'and 5'-gtgtagcccctgcttctcc-3' for rs7696323 typing and 5'-tcatttggcatcattggaaa-3' and 5'-gagttgcggcaaattcaaag-3' for rs3804100 typing. The PCR condition was 95°C 5 min followed by 35 cycles of 95°C 30 sec, 58°C or 53°C 30 sec for rs7696323 or rs3804100, respectively, and 72°C 30 sec, and a final extension step of 72°C 10 min. The PCR products were digested by BsrI and MwoI for rs7696323 and rs3804100 typing, respectively, followed by electrophoresis in 3% agarose gel. The Ins/Del typing was done by PCR with a primer pair, 5'-gcggactttccctttgct-3' and 5'-gtgcagagagaccacacgag-3' under

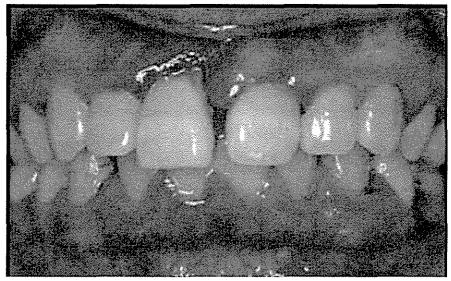

Fig. (1). A photograph of teeth from a typical AgP case. The patient was 23 years old. She was severely affected with swollen gum and almost losing the upper right incisor tooth.

the PCR condition described above, except that the annealing temperature was 57°C and electrophoresis was done in 2% agarose gel.

Statistical Analysis

Allele and genotype frequencies of the polymorphisms in the patients and controls were obtained by direct counting. Departure from Hardy-Weinberg equilibrium (HWE) was calculated by chi-square test. Statistical significance of differences between the AgP patients and control subjects were assessed by Mantel-Haenzel chi-square analysis, which was combined with the 2 x 2 contingency tables using the GraphPad in Stat software (GraphPad Software Inc., La Jolla, CA, USA). Fisher's exact test was used if the number of any cells of the 2 x 2 contingency table was <5. Relative risk with 95% confidence interval (CI) was calculated as the odds ratio. Linkage disequilibrium (LD) among the alleles of tested markers and their haplotype frequencies was estimated by using the Haploview program (Haploview 4.2, http://www.broad.mit.edu/mpg/haploview/index.php). Permutation test (n=5,000) was also performed by using Haploview. P values <0.05 were considered to be statistically significant.

RESULTS

Clinical parameters of enrolled AgP patients were shown in Table **1**. Every clinical data showed severe progression of periodontal disease at their ages. A typical AgP case is shown in Fig. (**1**). The patient was 23 years old female, who showed gum of swelling and redness, and her upper right incisor tooth almost came out. She had serious problems in her mouth, but had no systemic disease other than the severe periodontitis. The allele and genotype frequencies of tested markers are listed in Table **2**. It was found that the allele frequencies of Ins/Del alleles and T/C alleles of rs3804100 showed statistically significant associations with AgP, with p values 0.0022 and 0.0018, respectively, although these associations were not statistically significant after correction for multiple testing (Bonferroni's correction). Because there

Table 2. Case-Control Association Study of TLR2 Polymorphisms in Japanese AgP

Genetic Marker		Patient (n = 38)	Control (n = 190)	OR[#4]	95% CI[#5]	p
-196 to -174 Ins>Del						
genotype frequency[#1]	Ins/Ins	12 (31.6%)	87 (45.8%)			
	Ins/Del	17 (44.7%)	83 (43.7%)			
	Del/Del	9 (23.7%)	20 (10.5%)	2.64	1.09–6.36	0.026
	HWE[#3]	p = 0.83	p = 1.00			
Allele frequency[#2]	Ins	41 (53.9%)	257 (67.6%)	0.56	0.34–0.92	0.022
	Del	35 (46.1%)	123 (32.4%)	1.78	1.08–2.94	
rs7696323 C>T						
genotype frequency	C/C	20 (52.6%)	133 (70.0%)	0.48	0.23–0.97	0.038
	C/T	16 (42.1%)	49 (25.8%)			
	T/T	2 (5.3%)	8 (4.2%)			
	HWE	p = 0.87	p = 0.46			
Allele frequency	C	56 (73.7%)	315 (82.9%)	0.58		
	T	20 (26.3%)	65 (17.1%)	1.73		
rs3804100 T>C						
genotype frequency	T/T	12 (31.6%)	97 (51.1%)	0.44	0.21–0.93	0.028
	T/C	20 (52.6%)	78 (41.1%)			
	C/C	6 (15.8%)	15 (7.9%)			
	HWE	p = 0.89	p = 0.99			
Allele frequency	T	44 (57.9%)	272 (71.6%)	0.55	0.33–0.91	0.018
	C	32 (42.1%)	108 (28.4%)	1.83	1.10–3.04	

[#1, #2]Summation of genotype or allele frequencies at each locus may not be 1.00 because each frequency was rounded.

[#3]HWE; Hardy–Weinberg equilibrium.

[#4]Odds ratio

[#5]95% confidence interval was calculated when p value was less than 0.05.